Dynamics of HIV Neutralization by a Microbicide Formulation Layer: Biophysical Fundamentals and Transport Theory

Anthony R. Geonnotti* and David F. Katz*†
*Department of Biomedical Engineering, and †Department of Obstetrics and Gynecology, Duke University, Durham, North Carolina

ABSTRACT Topical microbicides are an emerging HIV/AIDS prevention modality. Microbicide biofunctionality requires creation of a chemical-physical barrier against HIV transmission. Barrier effectiveness derives from properties of the active compound and its delivery system, but little is known about how these properties translate into microbicide functionality. We developed a mathematical model simulating biologically relevant transport and HIV-neutralization processes occurring when semen-borne virus interacts with a microbicide delivery vehicle coating epithelium. The model enables analysis of how vehicle-related variables, and anti-HIV compound characteristics, affect microbicide performance. Results suggest HIV neutralization is achievable with postcoital coating thicknesses ~100 μm. Increased microbicide concentration and potency hasten viral neutralization and diminish penetration of infectious virus through the coating layer. Durable vehicle structures that restrict viral diffusion could provide significant protection. Our findings demonstrate the need to pair potent active ingredients with well-engineered formulation vehicles, and highlight the importance of the dosage form in microbicide effectiveness. Microbicide formulations can function not only as drug delivery vehicles, but also as physical barriers to viral penetration. Total viral neutralization with 100-μm-thin coating layers supports future microbicide use against HIV transmission. This model can be used as a tool to analyze diverse factors that govern microbicide functionality.

INTRODUCTION

The HIV pandemic continues to overwhelm current preventative measures at a rate of 12,000 new infections a day (1). Women account for a disproportionate number of these new infections. Most of the infected young people are aged 15–24 worldwide, and 59% of all infected adults in sub-Saharan Africa are female. In several African countries, prevalence rates for young women (ages 15–24) are over three times higher than their male counterparts (1). Increased biological vulnerability, combined with cultural and socioeconomic inequities, results in greater HIV susceptibility and, consequently, infections in women (2–4). New HIV prevention methods will benefit women by augmenting their abilities to manage their sexual health, thus protecting themselves and their communities.

Microbicide development is a response to this demonstrated need for new, female-controlled, methods for HIV prophylaxis (2–7). Topical vaginal microbicide dosage forms—which may take forms such as gels, creams, films, sponges, or rings—are intended to prevent transmission of HIV and/or other sexually introduced pathogens, providing women with safe, affordable, and cosmetically acceptable protection. Microbicides may function by disabling pathogens, hindering pathogen transport, protecting tissue from injury, inhibiting early infectious processes, or combinations of the above.

An effective microbicide may combine a potent active ingredient that neutralizes target pathogens with a well-engineered formulation vehicle that delivers the active ingredient while providing a barrier and lubrication layer. To date, the majority of microbicide research has focused on identifying, testing, and manufacturing the active compounds. However, there remain many unanswered questions about the role and importance of the delivery vehicle in microbicide efficacy. Several laboratories, including ours, have designed in vitro and in vivo experiments, and mathematical epithelial coating theories, to begin to understand the determinants of microbicide formulation distribution within the complex physiological vaginal environment (8–12). However, there has been very little investigation to date into the collective, quantitative impact that coating layer properties (e.g., extent, durability, thickness, structure) have on microbicide prophylactic efficacy.

Our goal here was to create a model that simulates relevant transport and HIV neutralization processes inherent in microbicide function, and to use that model to understand and predict the effects that several critical microbicide vehicle properties have on ultimate HIV prophylaxis in vivo. We develop a system of transport equations for both virus, originating in the semen, and a mobile anti-HIV agent, originating in an epithelial coating layer. These equations track the simultaneous migration of virus and microbicide while accounting for their interaction. We develop an expression for viral neutralization in terms of specific microbicide binding kinetics. The analysis in this initial study focuses on neutralization of HIV by a gp120 fusion inhibitor. Because the processes that neutralize HIV fusion must occur before epithelial contact—i.e., within the formulation/semen system—fusion inhibiting compounds were logical choices for this analysis. The protein Cyanovirin-N (CV-N) was chosen as an example fusion inhibitor due to the large amount of

Submitted April 5, 2006, and accepted for publication June 14, 2006.

Address reprint requests to Anthony Geonnotti, Box 90281, Durham, NC 27708. Tel.: 919-660-5414; E-mail: anthony.geonnotti@duke.edu.

0006-3495/06/09/2121/10 $2.00

doi: 10.1529/biophysj.106.086322

published research characterizing its activity and its current status as a promising microbicide (13–18). However, the conceptual mathematical framework used here is broadly applicable to a number of potential microbicide prophylactic mechanisms. Microbicide effectiveness—a function of factors specific to given formulated vehicles and active ingredients—can then be determined by examining the rate at which infectious virus reaches epithelial tissue.

MATERIALS AND METHODS

The interacting transport processes of HIV virions and microbicide molecules can be modeled by a two-compartment, two-component, one-dimensional, unsteady diffusion system with bimolecular viral neutralization terms (Fig. 1). We assume transmission from HIV-infected semen, existence of a uniform formulation coating layer over epithelium, and we focus on diffusive, postcoital transport of cell-free HIV. The assumption of one-dimensional diffusion is justified because the thicknesses of epithelial coating layers are typically very small compared to the lateral extents of those layers (8). Although cell-associated virus may play a role in HIV transmission, we have omitted its transport here because of its significantly lower rate of diffusion through a formulation layer. We track more the mobile cell-free virus because it will reach the epithelium sooner. This provides a conservative (i.e., lower bound) estimate of the time virus needs to cross the formulation layer.

Governing equations of transport

These equations characterize transport and reversible interactions of virus and generic mobile active ingredient within the semen-formulation system. They provide a foundation that we subsequently expand to incorporate neutralization kinetics for CV-N. Variable definitions and example values are given in Table 1.

$$\left.\begin{aligned}\frac{\partial C_V}{\partial t} &= D_{V_{semen}}\frac{\partial^2 C_V}{\partial x^2} - k_{f_{semen}}C_V C_M + k_{r_{semen}}C_N\\ \frac{\partial C_M}{\partial t} &= D_{M_{semen}}\frac{\partial^2 C_M}{\partial x^2} - k_{f_{semen}}C_V C_M + k_{r_{semen}}C_N\end{aligned}\right\}\quad -\varepsilon L \le x < 0 \tag{1}$$

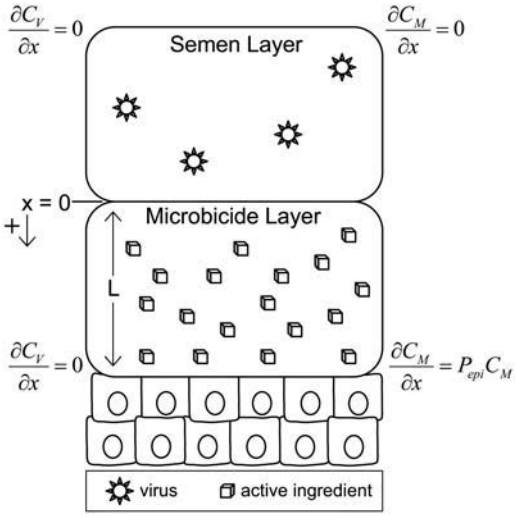

FIGURE 1 Geometry of model system.

$$\left.\begin{aligned}\frac{\partial C_V}{\partial t} &= D_{V_{gel}}\frac{\partial^2 C_V}{\partial x^2} - k_{f_{gel}}C_V C_M + k_{r_{gel}}C_N\\ \frac{\partial C_M}{\partial t} &= D_{M_{gel}}\frac{\partial^2 C_M}{\partial x^2} - k_{f_{gel}}C_V C_M + k_{r_{gel}}C_N\end{aligned}\right\}\quad 0 \le x \le L. \tag{2}$$

Boundary and initial conditions

We assume that no virus or microbicide leave or enter the system from the upper surface of the semen layer (Eq. 3). Physiologically, this boundary may be open to air; or a symmetric, inverted semen/formulation layer could be vertically adjacent to this system (i.e., we would be considering the bottom half of a symmetric system).

$$\frac{\partial C_V(-\varepsilon L,t)}{\partial x} = 0 \quad \frac{\partial C_M(-\varepsilon L,t)}{\partial x} = 0. \tag{3}$$

We apply standard concentration and flux boundary conditions at the semen-formulation interface (Eqs. 4 and 5).

$$C_V(0^+,t) = \Phi_V C_V(0^-,t) \quad C_M(0^+,t) = \Phi_M C_M(0^-,t) \tag{4}$$

$$D_{V_{gel}}\frac{\partial C_V(0^+,t)}{\partial x} = D_{V_{semen}}\frac{\partial C_V(0^-,t)}{\partial x}$$

$$D_{M_{gel}}\frac{\partial C_M(0^+,t)}{\partial x} = D_{M_{semen}}\frac{\partial C_M(0^-,t)}{\partial x}. \tag{5}$$

Beneath the formulation layer, mucosal epithelium presents a significant barrier to transport (5). We calculate the rate at which microbicide is transported into the epithelium using permeability values taken from relevant literature (19–21). Mechanisms by which HIV crosses the mucosal barrier are not well understood; however, we assume that the rate of transepithelial viral transport is much slower than the rate of viral transport within the formulation. This viral ''bottleneck'' (5) allows us to neglect viral permeability in our boundary conditions (Eq. 6). Infection can be understood as a consequence of the local concentration at the interface.

$$\frac{\partial C_V(L,t)}{\partial x} = 0 \quad \frac{\partial C_M(L,t)}{\partial x} = P_{epi}C_M. \tag{6}$$

Initially, all infectious virus is within the semen, and all microbicide is in the formulation layer (Eq. 7).

$$\left.\begin{aligned}C_V(x,0) &= C_{V_o}\\ C_M(x,0) &= 0\end{aligned}\right\}\quad for \quad -\varepsilon L \le x < 0$$

$$\left.\begin{aligned}C_V(x,0) &= 0\\ C_M(x,0) &= C_{M_o}\end{aligned}\right\}\quad for \quad 0 \le x \le L. \tag{7}$$

Viral neutralization kinetics

The viral neutralization term is of the form:

$$-k_f C_M C_V + k_r C_N. \tag{8}$$

This expression represents reversible binding and neutralization of one microbicide molecule to a virion. Neutralization kinetics are mechanism dependent, and will vary for given anti-HIV agents. We use the fusion inhibitor, Cyanovirin-N (CV-N), as an example microbicide to demonstrate our model. CV-N is an 11-kD protein that is derived from blue-green algae and neutralizes HIV by binding with high affinity to gp120, a glycoprotein projection on the virion's surface. This prevents gp120 from interacting with cellular CD4 and initiating fusion, thereby preventing infection (14–18). Studies of binding stoichiometry have suggested that up to 5 CV-N molecules may bind to a single soluble, nontrimeric, nonvirion associated gp120 (18). However, trimeric, virion-associated gp120 may exhibit different stoichiometry. It has been shown

TABLE 1 Relevant parameters and reference conditions

Variable	Definition	Reference conditions
C_{V0}	Initial virus concentration in semen	1.66×10^{-15} M
C_{Vi}	Virus with i CV-N bound	–
C_{M0}	Initial microbicide concentration in coating layer	1000.0×10^{-9} M
C_M	Microbicide concentration in coating layer	–
C_N	Neutralized virus concentration	–
D_{Vsemen}	Diffusion coefficient of virus in semen	6.49×10^{-9} cm^2 s^{-1}
D_{Vgel}	Diffusion coefficient of virus in coating layer	6.49×10^{-11} cm^2 s^{-1}
D_{Msemen}	Diffusion coefficient of microbicide in semen	1.72×10^{-7} cm^2 s^{-1}
D_{Mgel}	Diffusion coefficient of microbicide in coating layer	1.72×10^{-8} cm^2 s^{-1}
D_{CVN}	Diffusion coefficient of CV-N in a medium	–
D_{HIV}	Diffusion coefficient of HIV in a medium	–
k_{fsemen}	Forward kinetic constant in semen	4.72×10^6 M^{-1} s^{-1}
k_{rsemen}	Reverse kinetic constant in semen	4.7×10^{-3} s^{-1}
k_{fgel}	Forward kinetic constant in coating layer	4.57×10^5 M^{-1} s^{-1}
k_{rgel}	Reverse kinetic constant in coating layer	4.57×10^{-4} s^{-1}
L	Formulation thickness	100 μm
N_A	Avogadro's number	6.02×10^{23}
Φ_V,Φ_M	Semen/formulation partition coefficient	1
P_{epi}	Epithelial permeability to microbicide	10^{-6} cm s^{-1}
R_{HIV}	Radius of HIV	70 nm
R_{trimer}	Radius of gp120 trimer	7 nm
–	Dimensions of CV-N	55 × 25 Å

that approximately two CV-N molecules are needed to inhibit binding to cell-associated CD4 (14,17). Therefore, while a 5:1 CVN-gp120 ratio may be possible, 2:1 is sufficient to inhibit fusion.

Mature HIV displays ~10 gp120 trimers on its surface (22–26); all trimers must be blocked for neutralization (22,24,27). The presence of 10 glycoprotein trimers, each with three gp120s requiring two CV-N for inactivation, results in a maximum of 60 separate CV-N binding events per virion. Recent research has suggested that blocking two out of three gp120 per trimer is sufficient to inactivate a trimer (28). Therefore, 50 binding events must occur for HIV neutralization (i.e., each gp120 has one CV-N and 20 gp120s have at least two CV-N.)

We assume that binding is diffusion limited, and we apply collision theory to develop approximate association constants. This assumption is valid due to very low K_D (2–45 nM) values of CV-N and other current microbicidal compounds (18). Therefore, the molar rate of inactivation, assuming instantaneous binding upon collision for a virion with one glycoprotein stalk, is the product of CV-N flux to the virion ($C_{CVN}(D_{CVN}+D_{HIV})/\ R_{HIV}$) and the accessible hemispherical surface area of the active site ($2\pi R_{trimer}^2$). We find that:

$$\text{molar rate of binding for a single trimer} = \left[\frac{2\pi N_A (D_{CVN}+D_{HIV})R_{trimer}^2}{1000R_{HIV}}\right] C_{CVN}C_V. \quad (9)$$

Avogadro's number and division by 1000 were needed to convert from cgs units to molar quantities.

Calculations using the derived association constant (k_f)—the bracketed term in Eq. 9—compare very well with experimental values of CV-N binding to gp120 (14,18). Previously, BIACORE assays produced values of k_f in the 10^6 M^{-1}s^{-1} range, and k_r values around 10^{-3} s^{-1} (18). These studies may underestimate the true association constant, due to mass-transport limitations arising from slow diffusion of the large protein and from fast binding (29). Other titration studies have estimated the association constant to be around 2.4×10^7 M^{-1}s^{-1} (14). Note that these measurements were performed with soluble gp120, and were not tests for HIV neutralization.

Because 50 separate binding events must occur for actual HIV neutralization, the neutralization term (Eq. 8) must be expanded and adapted to include multiple binding events. Simultaneous or sequential binding models are not appropriate for this case. Therefore, we adapted a model employed by Perelson to describe multivalent receptors as a set of independent monovalent receptors (30). If we assume that the two separate binding sites on gp120 do not interact, due to the large size difference between CV-N and gp120 (11 vs. 120 kD), we have a set of 60 monovalent receptors (15,25). We can then use statistical kinetic theory to describe how small molecules bind to multiple identical binding sites (31). This results in a correction to the equilibrium constant to account for the number of free receptors before binding and the number of occupied receptors after binding. The dependence of previously bound receptors on the binding reaction is as follows (31):

$$(n-i+1)k_f C_{V_{i-1}} C_M \rightleftharpoons (i)k_r C_{V_i}, \quad (10)$$

where n is the total number of receptors and i is the number of bound receptors resulting from the reaction (i.e., the reaction is binding the ith site).

Each of the 60 receptors can exist in two states: bound and unbound. Our model accounts for 61 interconverting virus populations (i.e., HIV with 0 CV-N bound through 60 bound) in two separate compartments (semen and vehicle). Combined with tracking virus and microbicide in both compartments, this expands the model from 4 to 124 simultaneous equations. The model tracks virus and microbicide in space and time, identifying virus in various states of neutralization. A schematic of viral neutralization kinetics is shown in Fig. 2. Because the model distinguishes virions by the number of CV-N bound, the number of binding events per trimer needed to fully neutralize a virion (initially 5 CV-N per trimer) can be modified by simply changing the threshold at which that virion is counted as neutralized (i.e., all virus with less than 50 CV-N bound).

Complete nondimensionalized equations

Model transport equations (Eqs. 1 and 2) were nondimensionalized using the following transformations.

$$\tilde{x} = \frac{x}{L} \quad \tilde{C}_{V_i} = \frac{C_{V_i}}{C_{V_0}} \quad \tilde{t} = tk_f C_{M_0}, \quad (11)$$

where C_{V_i} is the concentration of virus with i CV-N bound, and C_{V_0} is the initial concentration of all virus.

Because microbicide concentration is many orders of magnitude larger than viral concentration (Table 1), we assume that any loss of microbicide due to viral binding is negligible. Not all 124 equations are shown, for compactness.

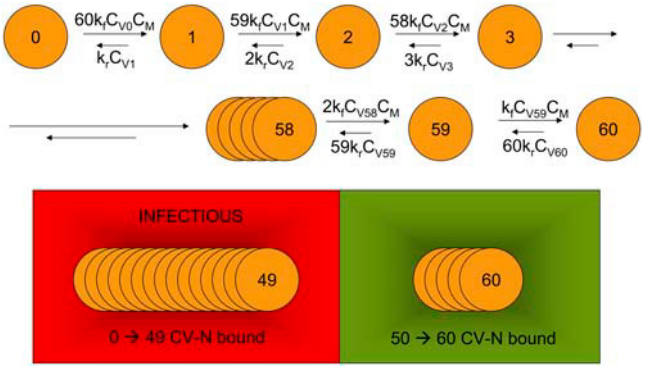

FIGURE 2 Schematic of viral neutralization kinetics.

Dimensionless equations within semen layer ($-\varepsilon \le x < 0$)

$$\frac{\partial \tilde{C}_{V_0}(x,t)}{\partial \tilde{t}} = \frac{D_{V_{semen}}}{k_{f_{gel}} C_{M_0} L^2}\frac{\partial^2 \tilde{C}_{V_0}(x,t)}{\partial \tilde{x}^2} - 60\frac{k_{f_{semen}}}{k_{f_{gel}}}\tilde{C}_{V_0}(x,t)\tilde{C}_M(x,t) + \frac{k_{r_{semen}}}{k_{f_{gel}} C_{M_0}}\tilde{C}_{V_1}(x,t)$$

$$\frac{\partial \tilde{C}_{V_1}(x,t)}{\partial \tilde{t}} = \frac{D_{V_{semen}}}{k_{f_{gel}} C_{M_0} L^2}\frac{\partial^2 \tilde{C}_{V_1}(x,t)}{\partial \tilde{x}^2} + 60\frac{k_{f_{semen}}}{k_{f_{gel}}}\tilde{C}_{V_0}(x,t)\tilde{C}_M(x,t) - \frac{k_{r_{semen}}}{k_{f_{gel}} C_{M_0}}\tilde{C}_{V_1}(x,t) - 59\frac{k_{f_{semen}}}{k_{f_{gel}}}\tilde{C}_{V_1}(x,t)\tilde{C}_M(x,t) + 2\frac{k_{r_{semen}}}{k_{f_{gel}} C_{M_0}}\tilde{C}_{V_2}(x,t)$$

$$\frac{\partial \tilde{C}_{V_2}(x,t)}{\partial \tilde{t}} = \frac{D_{V_{semen}}}{k_{f_{gel}} C_{M_0} L^2}\frac{\partial^2 \tilde{C}_{V_2}(x,t)}{\partial \tilde{x}^2} + 59\frac{k_{f_{semen}}}{k_{f_{gel}}}\tilde{C}_{V_1}(x,t)\tilde{C}_M(x,t) - 2\frac{k_{r_{semen}}}{k_{f_{gel}} C_{M_0}}\tilde{C}_{V_2}(x,t) - 58\frac{k_{f_{semen}}}{k_{f_{gel}}}\tilde{C}_{V_2}(x,t)\tilde{C}_M(x,t) + 3\frac{k_{r_{semen}}}{k_{f_{gel}} C_{M_0}}\tilde{C}_{V_3}(x,t)$$

.
.

$$\frac{\partial \tilde{C}_{V_{59}}(x,t)}{\partial \tilde{t}} = \frac{D_{V_{semen}}}{k_{f_{gel}} C_{M_0} L^2}\frac{\partial^2 \tilde{C}_{V_{59}}(x,t)}{\partial x^2} + 2\frac{k_{f_{semen}}}{k_{f_{gel}}}\tilde{C}_{V_{58}}(x,t) \times \tilde{C}_M(x,t) - 59\frac{k_{r_{semen}}}{k_{f_{gel}} C_{M_0}}\tilde{C}_{V_{59}}(x,t) - \frac{k_{f_{semen}}}{k_{f_{gel}}}\tilde{C}_{V_{59}}(x,t)\tilde{C}_M(x,t) + 60\frac{k_{r_{semen}}}{k_{f_{gel}} C_{M_0}}\tilde{C}_{V_{60}}(x,t)$$

$$\frac{\partial \tilde{C}_{V_{60}}(x,t)}{\partial \tilde{t}} = \frac{D_{V_{semen}}}{k_{f_{gel}} C_{M_0} L^2}\frac{\partial^2 \tilde{C}_{V_{60}}(x,t)}{\partial \tilde{x}^2} + \frac{k_{f_{semen}}}{k_{f_{gel}}}\tilde{C}_{V_{59}}(x,t)\tilde{C}_M(x,t) - 60\frac{k_{r_{semen}}}{k_{f_{gel}} C_{M_0}}\tilde{C}_{V_{60}}(x,t)$$

$$\frac{\partial \tilde{C}_M(x,t)}{\partial \tilde{t}} = \frac{D_{M_{semen}}}{k_{f_{gel}} C_{M_0} L^2}\frac{\partial^2 \tilde{C}_M(x,t)}{\partial \tilde{x}^2}. \tag{12}$$

Dimensionless equations within formulation layer ($0 < x \le 1$)

$$\frac{\partial \tilde{C}_{V_0}(x,t)}{\partial \tilde{t}} = \frac{D_{V_{gel}}}{k_{f_{gel}} C_{M_0} L^2}\frac{\partial^2 \tilde{C}_{V_0}(x,t)}{\partial \tilde{x}^2} - 60\tilde{C}_{V_0}(x,t)\tilde{C}_M(x,t) + \frac{k_{r_{gel}}}{k_{f_{gel}} C_{M_0}}\tilde{C}_{V_1}(x,t)$$

$$\frac{\partial \tilde{C}_{V_1}(x,t)}{\partial \tilde{t}} = \frac{D_{V_{gel}}}{k_{f_{gel}} C_{M_0} L^2}\frac{\partial^2 \tilde{C}_{V_1}(x,t)}{\partial \tilde{x}^2} + 60\tilde{C}_{V_0}(x,t)\tilde{C}_M(x,t) - \frac{k_{r_{gel}}}{k_{f_{gel}} C_{M_0}}\tilde{C}_{V_1}(x,t) - 59\tilde{C}_{V_1}(x,t)\tilde{C}_M(x,t) + 2\frac{k_{r_{gel}}}{k_{f_{gel}} C_{M_0}}\tilde{C}_{V_2}(x,t)$$

$$\frac{\partial \tilde{C}_{V_2}(x,t)}{\partial \tilde{t}} = \frac{D_{V_{gel}}}{k_{f_{gel}} C_{M_0} L^2}\frac{\partial^2 \tilde{C}_{V_2}(x,t)}{\partial \tilde{x}^2} + 59\tilde{C}_{V_1}(x,t)\tilde{C}_M(x,t) - 2\frac{k_{r_{gel}}}{k_{f_{gel}} C_{M_0}}\tilde{C}_{V_2}(x,t) - 58\tilde{C}_{V_2}(x,t)\tilde{C}_M(x,t) + 3\frac{k_{r_{gel}}}{k_{f_{gel}} C_{M_0}}\tilde{C}_{V_3}(x,t)$$

.
.

$$\frac{\partial \tilde{C}_{V_{59}}(x,t)}{\partial \tilde{t}} = \frac{D_{V_{gel}}}{k_{f_{gel}} C_{M_0} L^2}\frac{\partial^2 \tilde{C}_{V_{59}}(x,t)}{\partial x^2} + 2\tilde{C}_{V_{58}}(x,t)\tilde{C}_M(x,t) - 59\frac{k_{r_{gel}}}{k_{f_{gel}} C_{M_0}}\tilde{C}_{V_{59}}(x,t) - \tilde{C}_{V_{59}}(x,t)\tilde{C}_M(x,t) + 60\frac{k_{r_{gel}}}{k_{f_{gel}} C_{M_0}}\tilde{C}_{V_{60}}(x,t)$$

$$\frac{\partial \tilde{C}_{V_{60}}(x,t)}{\partial \tilde{t}} = \frac{D_{V_{gel}}}{k_{f_{gel}} C_{M_0} L^2}\frac{\partial^2 \tilde{C}_{V_{60}}(x,t)}{\partial \tilde{x}^2} + \tilde{C}_{V_{59}}(x,t)\tilde{C}_M(x,t) - 60\frac{k_{r_{gel}}}{k_{f_{gel}} C_{M_0}}\tilde{C}_{V_{60}}(x,t)$$

$$\frac{\partial \tilde{C}_M(x,t)}{\partial \tilde{t}} = \frac{D_{M_{gel}}}{k_{f_{gel}} C_{M_0} L^2}\frac{\partial^2 \tilde{C}_M(x,t)}{\partial \tilde{x}^2}. \tag{13}$$

Dimensionless boundary conditions (adapted from Eqs. 3–6)

No transport from semen layer:

$$\frac{\partial \tilde{C}_{V_i}(-\varepsilon,\tilde{t})}{\partial \tilde{x}} = 0 \quad \frac{\partial \tilde{C}_M(-\varepsilon,\tilde{t})}{\partial \tilde{x}} = 0. \tag{14}$$

Semen-vehicle interface:

$$\tilde{C}_{V_i}(0^+,\tilde{t}) = \Phi_V \tilde{C}_{V_i}(0^-,\tilde{t}) \quad \tilde{C}_M(0^+,\tilde{t}) = \Phi_M \tilde{C}_M(0^-,\tilde{t}) \tag{15}$$

$$\frac{\partial \tilde{C}_{V_i}(0^+,\tilde{t})}{\partial \tilde{x}} = \frac{D_{V_{semen}}}{D_{V_{gel}}}\frac{\partial \tilde{C}_{V_i}(0^-,\tilde{t})}{\partial \tilde{x}}$$

$$\frac{D_{M_{gel}}}{D_{V_{gel}}}\frac{\partial \tilde{C}_M(0^+,\tilde{t})}{\partial \tilde{x}} = \frac{D_{M_{semen}}}{D_{V_{gel}}}\frac{\partial \tilde{C}_M(0^-,\tilde{t})}{\partial \tilde{x}}. \tag{16}$$

Epithelium impermeable to virus, slightly permeable to microbicide:

$$\frac{\partial \tilde{C}_{V_i}(1,\tilde{t})}{\partial \tilde{x}} = 0 \quad \frac{\partial \tilde{C}_M(1,\tilde{t})}{\partial \tilde{x}} = \frac{P_{epi}L}{D_{Mg}}\tilde{C}_M. \tag{17}$$

Dimensionless initial conditions (adapted from Eq. 7)

All virus unbound and in semen; all microbicide in vehicle:

$$\left.\begin{array}{l}\tilde{C}_{V_0}(\tilde{x},0) = 1\\ \tilde{C}_{V_{i>0}}(\tilde{x},0) = 0\\ \tilde{C}_M(\tilde{x},0) = 0\end{array}\right\} \quad for \quad -\varepsilon \le \tilde{x} < 0$$

$$\left.\begin{array}{l}\tilde{C}_{V_i}(\tilde{x},0) = 0\\ \tilde{C}_M(\tilde{x},0) = 1\end{array}\right\} \quad for \quad 0 \le \tilde{x} \le 1. \tag{18}$$

System parameters (Table 1)

Concentrations of virus and microbicide

Viral load in human semen can reach concentrations of over 10^6/ml (1.66×10^{-15} M). Here, we have conservatively applied this relatively high viral concentration for humans, to maximally challenge the microbicide vehicle (32,33).

Initial microbicide concentrations within a drug delivery vehicle are likely to be orders of magnitude higher than seminal viral concentrations, due to the low molar concentration of virus in semen. Because CV-N has nanomolar potency, actual formulation loading will most likely be in the micromolar range. Here we consider both a micromolar concentration, as well as a 100-fold reduction in that concentration, to demonstrate concentration effects on viral neutralization.

Diffusion coefficients of virions and microbicide molecules

We are modeling postcoital transport within the semen-vehicle system as diffusion dominated. Assuming semen to be a Newtonian fluid with viscosity 5 cP (34), we estimate the diffusion coefficients of virus and anti-HIV particles in the semen using the Stokes-Einstein equation (26). The diffusion coefficient of an HIV virion in semen ($D_{V_{semen}} = 6.49\times10^{-9}\text{cm}^2\text{s}^{-1}$) at 37°C is calculated for a 70-nm radius sphere, whereas the diffusion coefficient of the microbicide molecule CV-N ($D_{M_{semen}} = 1.72\times10^{-7}\text{cm}^2\text{s}^{-1}$) is calculated for a prolate spheroid with major axis 55 Å and minor axis 25 Å (14,35). Note that the larger size of the virion results in a diffusion coefficient that is over 25 times smaller than that of the microbicidal molecule (Table 1).

Particle transport (virion, microbicide) through the microbicide vehicle coating layer may be restricted, in comparison to semen, due to the vehicle's molecular microstructure. Diffusion coefficients in the vehicle for both virus (D_{Vg}) and microbicide (D_{Mg}) will vary depending upon local vehicle properties, which may change with time and space. Little is currently known about restricted diffusion of HIV or CV-N; we consider high and low values of estimated diffusion coefficients to bracket biologically relevant ranges for both virus and microbicide. The high values for both particles derive from assuming no restriction of particle transport by the vehicle versus semen. The low values restrict diffusion 100-fold for the larger virus and 10-fold for the smaller CV-N. These values are approximations based on studies of diffusion of similar particles in hydrogels (36). Diffusion coefficients remain constant throughout the vehicle in this initial model.

Epithelial permeability

A multilayered stratified squamous epithelium exists along the vagina and ectocervix. This tissue transforms to a tight-junction columnar epithelium at the entrance to the cervical canal. There have been a number of studies on the permeability of epithelium to various compounds. Human cervical and vaginal epithelium have been shown to have permeability coefficients between 0.5×10^{-6} and 22×10^{-6} cm/s for relatively hydrophilic substances, ranging in size from tritiated water to 10 kD polydextrans (19–21,37). Cervical epithelium is slightly more permeable, as expected given its structure. Other studies on buccal, sublingual, and corneal tissue in pigs and rabbits have found similar permeability values (38–41). Here we consider examples in which permeability of epithelium to CV-N is $\sim10^{-6}$cm/s. HIV permeability is assumed to be negligible due to its larger size, resulting in a no-flux condition on viral transport. Physiologically, this results in the total amount of virus in the system remaining constant. Because the analysis here is primarily concerned with whether any infectious virus reaches the epithelial surface, the consequences of this assumption, namely, a slightly higher viral concentration at the boundary at very long times and the lack of quantification of viral transport into the epithelial compartment, do not affect the analysis of the results.

Layer thickness

The thickness (L) of the microbicide vehicle coating layer most likely ranges from nearly 0 to $\sim$1000 μm, depending on the amount inserted and its subsequent interactions within the vaginal environment. We used 100 μm as a reference value for computations and initially assumed equal thicknesses for both the semen and microbicide coating layer.

Partition coefficient

Because many hydrogel formulations are hydrophilic and have high water content, the semen/vehicle interface will very quickly become indistinct. Here we assume the partition coefficient to be unity. This is a conservative estimate and may overestimate the amount of virus that enters the vehicle coating layer.

RESULTS

The set of 124 simultaneous transport equations was evaluated using the partial differential equation solver, ''pdepe'', found in MATLAB (The Mathworks, Natick, MA). Outputs give concentrations of virus (in various states of neutralization) and of microbicide as functions of time and space, and of system properties, including: viral load in semen, microbicide concentration/potency, binding kinetics, thicknesses of microbicide vehicle and semen layers, and mobilities of virus and microbicide in those layers. The model was initially applied to a set of reference conditions (Table 1) to provide a baseline for subsequent comparisons. Initially, semen and vehicle layers are the same thickness, and the vehicle is assumed to restrict diffusion. Several factors, including microbicide concentration, viral and microbicide mobility, and layer thickness were then altered, and their effects analyzed and interpreted.

Reference conditions

Fig. 3 *A* shows infectious virus within the semen layer. Under the reference conditions, the microbicide diffuses into and neutralizes virus within semen before any infectious virus enters the vehicle layer. Fig. 3 *B* depicts the same

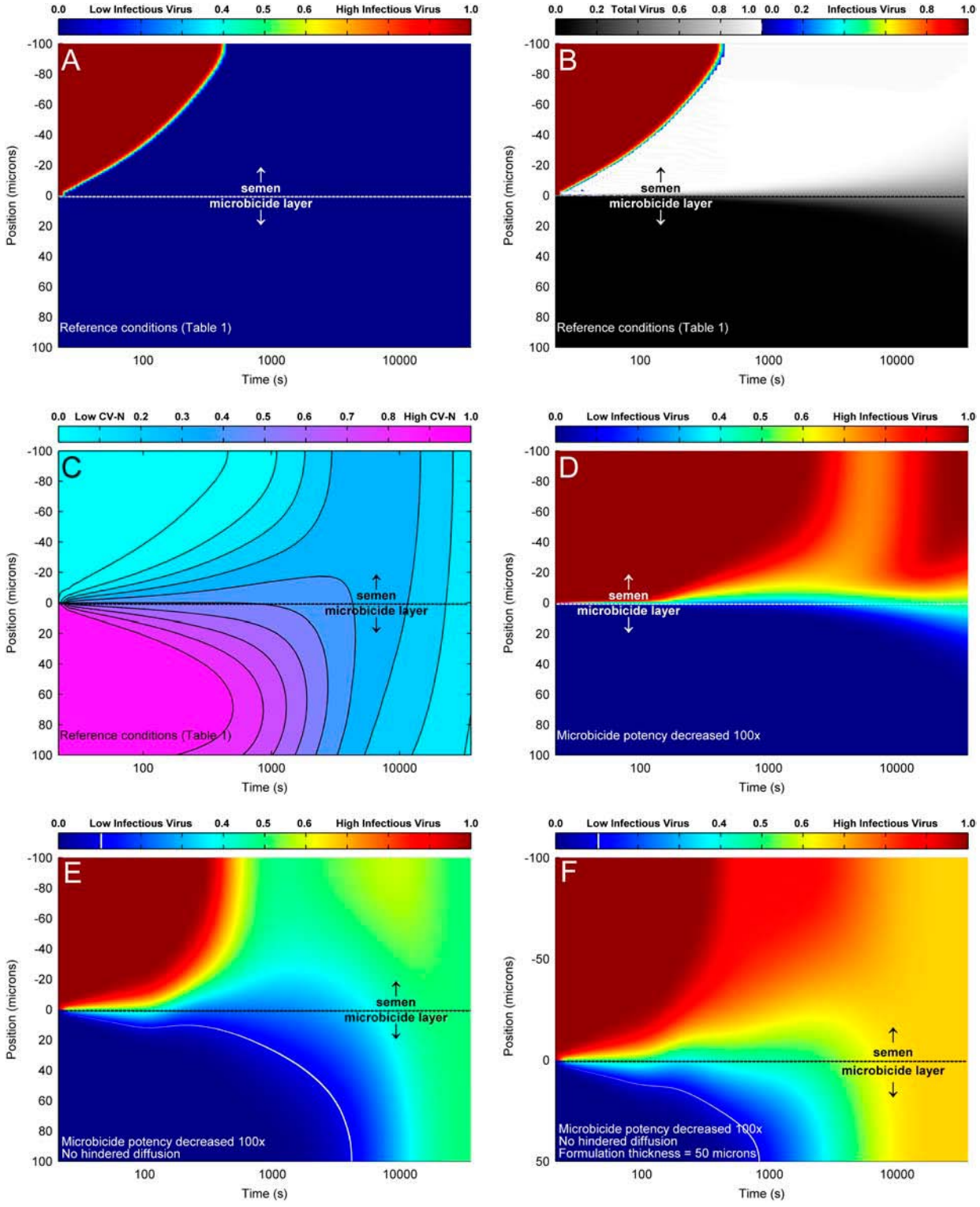

FIGURE 3 Viral neutralization model outputs. The top ($-100 \rightarrow 0$ μm) is semen layer, and the bottom ($0 \rightarrow 100$ μm) is formulation layer. Color-bar denotes concentration values relative to initial concentration. (*A*) Infectious virus concentration; reference conditions. (*B*) Total (*grayscale*) and infectious (*color*) virus concentration; reference conditions. (*C*) Microbicide concentration; reference conditions. (*D*) Infectious virus concentration; microbicide potency reduced 100×. (*E*) Infectious virus concentration; microbicide potency reduced 100× and viral and microbicide transport unhindered. (*F*) Infectious virus concentration; microbicide potency reduced 100×, viral and microbicide transport unhindered, and 50 μm formulation thickness. White line in panels *E* and *F* denotes 1 log reduction from seminal viral load.

conditions, but shows the transport of all virus; although virus begins to penetrate the layer within a few minutes, it has already been neutralized by the microbicide.

Distribution of the microbicide compound under the reference conditions is shown in Fig. 3 *C*. The microbicide diffuses into the semen where it neutralizes HIV. Due to the higher absolute concentration of microbicide as compared to virus, even a relatively small concentration of microbicide can have a significant effect on virus neutralization. Note that microbicide is continually being lost to epithelium and its concentration in the vehicle is markedly decreased within an hour.

Less potent active ingredient

Modifying parameters in the reference conditions, we illustrate the sensitivity of HIV neutralization kinematics to several critical properties of the microbicide delivery vehicle system. Fig. 3 *D* illustrates the effect of a less potent active ingredient, i.e., here we have reduced k_r/k_f by 100×. The microbicide is not able to neutralize the virus within the semen layer, and at longer times infectious virus begins to infiltrate the vehicle layer, although its transport is still hindered by the vehicle. Note in Eqs. 12 and 13 that an equal magnitude drop of initial microbicide concentration would have an identical effect because of the $(k_{r_{gel}}/k_{f_{gel}}C_{M_0})$ term in the governing equations.

Unrestricted diffusion

In all the previous examples, both viral and microbicide transport were hindered by the vehicle layer as compared to semen. Depending on the microstructure of the vehicle, this might not always be the case. That is, if a vehicle were not engineered for the vaginal environment, the process of dilution, and subsequent swelling, may change its microstructure and reduce its restrictive effect on particle diffusion. Fig. 3 *E* shows the same conditions as in Fig. 3 *D*, except that there is no restriction of diffusion, and the viral particles have the same mobility both in semen and the vehicle. Note that, in the absence of restricted diffusion, a previously adequate coating layer (with a given concentration and potency) becomes ineffective. Infectious virus concentration rises quickly at the epithelial surface.

Unrestricted diffusion plus a thinner formulation layer

As the microbicide vehicle layer becomes thinner, its effectiveness begins to be compromised. Fig. 3 *F* shows the same conditions as Fig. 3 *E*, but the vehicle thickness is halved to 50 μm. As expected, infectious HIV is able to traverse the vehicle layer more quickly. A more rapid loss of microbicide to the epithelium from such a thin layer further exacerbates the situation. This scenario represents a microbicide layer that has been rendered ineffective due to dilution and diminished thickness.

SENSITIVITY ANALYSIS

This analysis is originally based on the assumption that each virion has ~10 glycoprotein trimers projecting from its surface. This number of trimers represents an average value and may vary both within a given population of virus and between viral stocks. Therefore, we investigated whether variation in trimer number affected our results. We modified the model (by shrinking or expanding the number of equations) to represent a virus population with a 50% increase or decrease in the number of trimers (i.e., virus with five or 15 trimers versus the original 10). We compared results among the different cases by evaluating both concentration profiles of infectious virus and summary measures that give the times needed for either total neutralization of virus or for initial viral-epithelial contact. In all cases studied, the change in the number of trimers had very minimal effect on the results of the computations. Compared to the much higher microbicide concentration, this relatively small increase or decrease in the number of receptors (trimers) was negligible. Fig. 4 shows a representative case for the reference conditions.

We also wished to test the assumption that five binding events per trimer are needed for viral inactivation. This can be changed by simply increasing or decreasing the neutralization threshold that defines virus as infectious or neutralized. Because trimer number does not influence results, we tested three different neutralization conditions for the 10 trimer case—3, 4, and 5 CV-N per trimer. This corresponds to 30, 40, and 50 binding events, respectively. The results are

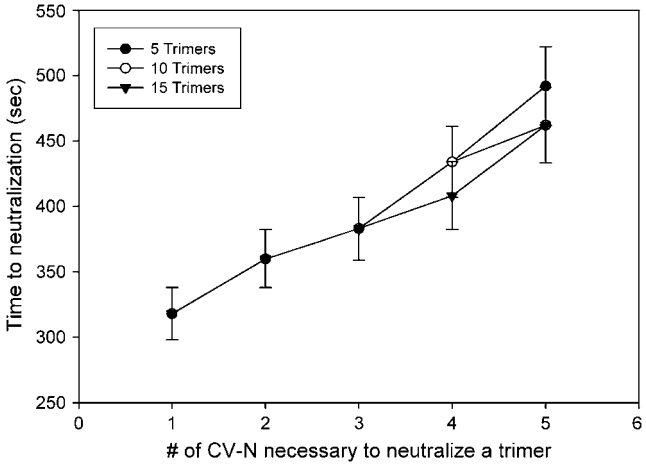

FIGURE 4 Model insensitivity to trimer number. Time to total viral neutralization is shown for three different trimer populations. Model conditions are the reference conditions used in Fig. 3, *A–C*. Error bars represent the temporal mesh size used in the MATLAB analysis and show the uncertainty inherent in the solution. Each case is present for all points; most points overlap and are indistinguishable from each other.

shown in Fig. 5. Decreasing binding events increased microbicide effectiveness. These results are not surprising, because a decrease in binding events is analogous to increasing microbicide potency or concentration, and the virus becomes easier to neutralize. The resurgence of infectious virus at longer times is due to the combined effects of: 1), a decreased microbicide concentration because of loss due to finite epithelial permeability; and 2), the reversible binding kinetics of CV-N. This highlights a possible advantage for microbicide compounds that irreversibly inactivate virus.

DISCUSSION

We have developed a dynamic HIV neutralization model that is applicable to a number of HIV/AIDS prophylaxis contexts, especially microbicide vehicle functionality. The model demonstrates interactive effects of several salient active ingredient and vehicle-specific parameters. We characterize microbicide vehicle effectiveness in relation to the local concentration of infectious virus that reaches the epithelial surface. Various measures of prophylactic failure can be defined with respect to this concentration. For example, in this analysis, we defined a measure of microbicide failure as the time at which infectious virus was present at the epithelium at a concentration $>10\%$ of the initial viral concentration. To facilitate the identification of this failure point, an iso-concentration line was drawn in white on the plots denoting a value of infectious virus concentration one log lower than the seminal viral load (see Fig. 3, *E* and *F*). This analysis also highlights the importance of the dosage form in microbicide effectiveness, especially its ability to restrict diffusion and resist erosion (Fig. 3, *D*–F). Decreased viral mobilities increase viral residence times within the delivery system, allowing total neutralization by moderately potent active compounds long before epithelial contact. Degradation of the coating layer before HIV neutralization severely compromises its ability to provide protection. Outputs from this model suggest that the thickness of an effective microbicide vehicle coating layer could realistically be on the order of 100 μm.

Different concentration profiles of virus, illustrated in Fig. 3, are consistent with distinctions in values of the diffusion coefficients (virus and active ingredient) between the semen and microbicide layers, in relation to potency of the microbicide. This is especially apparent in Fig. 3, *A* and *B*, which illustrate the vehicle's restrictive effect on viral mobility, coupled to rapid escape of microbicide into semen. This produces steep concentration gradients of viable virus near the semen-vehicle layer interface. In this model, coating thickness depicts the postcoital state of a vehicle that has been within the vaginal environment and exposed to ambient fluids, possibly for a number of hours. We recognize that the true semen-microbicide interface will not remain discrete over time: hydration of the vehicle layer will cause a time-dependent increase in the diffusion coefficient of the virus. This phenomenon is easily incorporated into the model by introducing spatial and temporal variability in the viral diffusion coefficient. It is also possible to include augmented mobilities of the virus and microbicide due to intravaginal forces (e.g., epithelial squeezing and coital shearing) that induce formulation flow. Simplifications of this initial model notwithstanding, the results here, which emphasize upper and lower bounds of viral permeability within microbicide delivery vehicle layers, are a mechanistically derived and useful guide for interpreting the efficacy of viral neutralization.

The prospect that a 100-μm-thick microbicide coating layer can be prophylactic against HIV transmission motivates development of dosage forms that optimize vaginal distribution and drug delivery around the creation and persistence of such thin layers. For perspective, applied volumes of current prototype vaginal microbicide gels range from ~2–4 ml. The surface area of the human vagina is likely to be $\leq$100 cm^2 (42). Thus, an average coating thickness would be $\geq$200 μm. Many factors determine the actual spatial distribution of coating, which is not likely to be uniformly thick or homogeneous in integrity (8). Nonetheless, the results here provide credibility to the notion that microbicide coating can function to block transport of infectious virus to vulnerable vaginal epithelium. They also

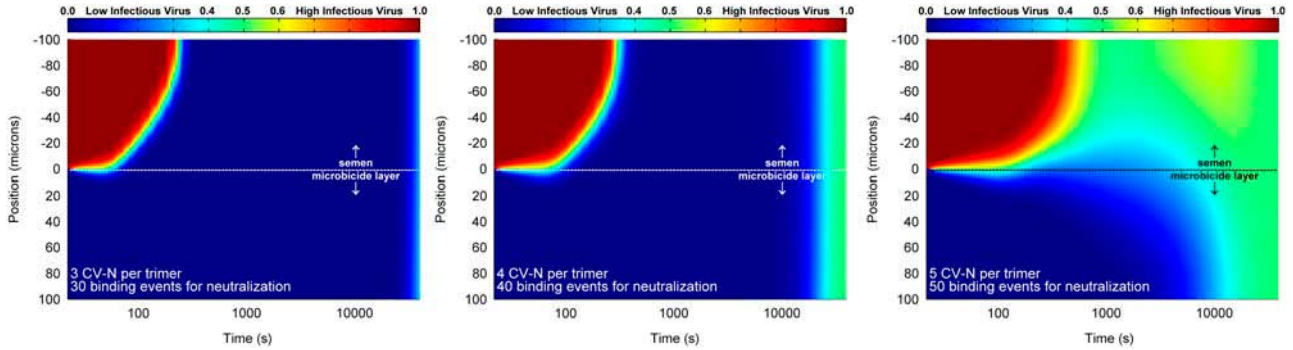

FIGURE 5 Effect of changing neutralization threshold. Figures show same conditions (no viral restriction, decreased microbicide concentration) as in Fig. 3 *E*, except with different neutralization conditions.

suggest that biologically incisive imaging of coating layers in vivo should employ modalities that can resolve coating thicknesses of the order of tens of microns (8). We note that there is also interest in microbicide application to the rectum, which presents a much larger vulnerable tissue surface area than the vagina. Here, the local prophylactic capability of 100 μm coating would remain possible; but the feasibility of achieving such coating over the much larger vulnerable surface area is uncertain.

Our virus neutralization model provides a framework for defining, measuring, and interpreting a set of critical phenomena that collectively govern microbicide product functionality. These include: binding kinetics between newly developed entry inhibitors and trimeric, virion associated gp120; compound-specific data on the kinetics, stoichiometry, and irreversibility of HIV neutralization; epithelial permeability to anti-HIV compounds; and diffusion coefficients of HIV in test vehicles (whole and during hydration by ambient vaginal fluids). The model enables rational, quantitative analysis of tradeoffs in effects of these determinants of microbicide prophylaxis. The geometry of the model is biologically relevant to in vivo distributions of HIV and microbicide, and serves to emphasize the need for experimental analyses of microbicides that embody similar configurations. That is, in vitro bioassays of microbicide potency should include configurations that resemble the basic multilayer structure that originates in vivo and that is embodied in our model: semen + microbicide vehicle + epithelium. Indeed, a powerful component in microbicide development would be linkage of results of such experiments with predictions of models such as ours. Additionally, this analysis has demonstrated the need for quantitative measurements of particle mobility within potential drug delivery vehicles. These experiments are currently ongoing in our lab and will eventually be incorporated into the analysis and design of future dosage forms.

Understanding factors that enhance or detract from particle transport would also benefit the design of future dosage for placebos for microbicide clinical trials. Such placebos should have the same distribution and retention behavior as the test microbicide products, and should also have minimal impact on HIV transmission. Achievement of the former may not be trivial. (12,43) Moreover, the transport model here has reinforced this need for valid placebos in clinical trials (44,45), because the results clearly show any diffusive restriction by a placebo coating layer would substantially increase viral residence time within the vagina, thereby exposing it to the body's natural defenses (low pH, hydrogen peroxide, innate antiviral proteins, etc.) and possibly provide a protective effect. (5,45) Any anti-HIV efficacy by placebo would have serious consequences in a randomized, controlled, clinical trial, because it would reduce the difference between the prophylactic effects of the test product and its control.

In general, the effects of factors such as microbicide potency, seminal viral load, layer thickness, mobility, etc. have nonlinear multivariate impacts on the kinematics of viral neutralization. Empirical, experimental delineation of such impacts would be a daunting task, but models of the type presented here provide a rational guide to such understanding.

We thank Mr. Douglas Kieweg and Dr. Sarah Kieweg for assistance with MATLAB programming. Thanks also to Matthew Furlow for completing the sensitivity analysis. We appreciate the critical reviews and insights provided by Drs. Patrick Kiser, David Montefiori, George Truskey, and Fan Yuan.

Financial support was provided by National Institutes of Health grant AI48103.

REFERENCES

1. UNAIDS. 2006. AIDS Epidemic Update. UNAIDS, Geneva, Switzerland.
2. Brown, H. 2004. Marvellous microbicides. *Lancet*. 363:1042–1043.
3. Shattock, R., and S. Solomon. 2004. Microbicides—aids to safer sex. *Lancet*. 363:1002–1003.
4. Stone, A. 2002. Microbicides: a new approach to preventing HIV and other sexually transmitted infections. *Nat. Rev. Drug Discov*. 1: 977–985.
5. Haase, A. T. 2005. Perils at the mucosal front lines for HIV and SIV and their hosts. *Nature Rev. Immunol*. 5:783–792.
6. Lard-Whiteford, S. L., D. Matecka, J. J. O'Rear, I. S. Yuen, C. Litterst, and P. Reichelderfer. 2004. Recommendations for the nonclinical development of topical microbicides for prevention of HIV transmission: an update. *J. Acquir. Immune Defic. Syndr*. 36: 541–552.
7. Moore, J. P., and R. Shattock. 2003. Preventing HIV-1 sexual transmission—not sexy enough science, or no benefit to the bottom line? *J. Antimicrob. Chemother*. 52:890–892.
8. Henderson, M. H., J. J. Peters, D. K. Walmer, G. M. Couchman, and D. F. Katz. 2005. An optical instrument for measurement of vaginal coating thickness by drug delivery formulations. *Rev. Sci. Instrum*. 76:1–7.
9. Garg, S., K. R. Tambwekar, K. Vermani, R. Kandarapu, A. Garg, D. P. Waller, and L. J. D. Zaneveld. 2003. Development pharmaceutics of microbicide formulations. Part II. Formulation, evaluation, and challenges. *Aids Patient Care STDS*. 17:377–400.
10. Kieweg, S. L., A. R. Geonnotti, and D. F. Katz. 2004. Gravity-induced coating flows of vaginal gel formulations: *In vitro* experimental analysis. *J. Pharm. Sci*. 93:2941–2952.
11. Pretorius, E. S., K. Timbers, D. Malamud, and K. Barnhart. 2002. Magnetic resonance imaging to determine the distribution of a vaginal gel: before, during, and after both simulated and real intercourse. *Contraception*. 66:443–451.
12. Geonnotti, A. R., J. J. Peters, and D. F. Katz. 2005. Erosion of microbicide formulation coating layers: effects of contact and shearing with vaginal fluid and semen. *J. Pharm. Sci*. 94:1705–1712.
13. Alliance for Microbiocide Development. 2005. Monthly Microbicide Pipeline Update. *Weekly News Digest* 6:2.
14. Bewley, C. A., and S. Otero-Quintero. 2001. The potent anti-HIV protein cyanovirin-N contains two novel carbohydrate binding sites that selectively bind to man(8) D1D3 and man(9) with nanomolar affinity: implications for binding to the HIV envelope protein gp120. *J. Am. Chem. Soc*. 123:3892–3902.
15. Boyd, M. R., K. R. Gustafson, J. B. McMahon, R. H. Shoemaker, B. R. O'Keefe, T. Mori, R. J. Gulakowski, L. Wu, M. I. Rivera, C. M. Laurencot, M. J. Currens, J. H. I. Cardellina, et al. 1997. Discovery of cyanovirin-N, a novel human immunodeficiency virus-inactivating protein that binds viral surface envelope glycoprotein sp120: potential

applications to microbicide development. *Antimicrob. Agents Chemother.* 41:1521–1530.

16. D'Cruz, O. J., and F. M. Uckun. 2004. Clinical development of microbicides for the prevention of HIV infection. *Curr. Pharm. Des.* 10:315–336.
17. Mori, T., and M. R. Boyd. 2001. Cyanovirin-N, a potent human immunodeficiency virus-inactivating protein, blocks both CD4-dependent and CD4-independent binding of soluble gp120 (sgp120) to target cells, inhibits sCD4-induced binding of sgp120 to cell-associated CXCR4, and dissociates bound sgp120 from target cells. *Antimicrob. Agents Chemother.* 45:664–672.
18. O'Keefe, B. R., S. R. Shenoy, D. Xie, W. Zhang, J. M. Muschnik, M. J. Currens, I. Chaiken, and M. R. Boyd. 2000. Analysis of the interaction between the HIV-inactivating protein Cyanovirin-N and soluble forms of the envelope glycoproteins gp120 and gp41. *Mol. Pharmacol.* 58:982–992.
19. Gorodeski, G. I. 2001. Vaginal-cervical epithelial permeability decreases after menopause. *Fertil. Steril.* 76:753–761.
20. Gorodeski, G. I. 2005. Aging and estrogen effects on transcervical-transvaginal epithelial permeability. *J. Clin. Endrocrinol. Metab.* 90: 345–351.
21. Gorodeski, G. I., M. F. Romero, U. Hopfer, E. Rorke, W. H. Utian, and R. L. Eckert. 1994. Human uterine cervical epithelial cells grown on permeable support—a new model for the study of differentiation and transepithelial transport. *Differentiation.* 56:107–118.
22. Yang, X., S. Kurteva, X. Ren, S. Lee, and J. Sodroski. 2005. Stoichiometry of envelope glycoprotein trimers in the entry of human immunodeficiency virus type 1. *J. Virol.* 79:12132–12147.
23. Gelderblom, H. R., E. H. S. Hausmann, M. Ozel, G. Pauli, and M. A. Koch. 1987. Fine structure of human immunodeficiency viruses and immunolocalization of structural proteins. *Virology.* 156:171–176.
24. Poignard, P., E. O. Saphire, P. W. Parren, and D. R. Burton. 2001. GP120: biologic aspects of structural features. *Annu. Rev. Immunol.* 19: 253–274.
25. Chertova, E., J. Bess, B. J. Crise, R. C. Sowder, T. M. Schaden, J. M. Hilburn, J. A. Hoxie, R. E. Benveniste, J. D. Lifson, L. E. Henderson, and L. O. Arthur. 2002. Envelope glycoprotein incorporation, not shedding of surface envelope glycoprotein (gp120/SU), is the primary determinant of SU content of purified human immunodeficiency virus type 1 and simian immunodeficiency virus. *J. Virol.* 76:5315–5325.
26. Zhu, P., E. Chertova, J. Bess, J. D. Lifson, L. O. Arthur, J. Liu, K. A. Taylor, and K. H. Roux. 2003. Electron tomography analysis of envelope glycoprotein trimers on HIV and simian immunodeficiency virus virions. *Proc. Natl. Acad. Sci. USA.* 100:15812–15817.
27. Yang, X., S. Kurteva, S. Lee, and J. Sodroski. 2005. Stoichiometry of antibody neutralization of human immunodeficiency virus type 1. *J. Virol.* 79:3500–3508.
28. Yang, X., S. Kurteva, X. Ren, S. Lee, and J. Sodroski. 2006. Subunit stoichiometry of human immunodeficiency virus type 1 envelope glycoprotein trimers during virus entry into host cells. *J. Virol.* 80:4388–4395.
29. Myszka, D. G., X. He, M. Dembo, T. A. Morton, and B. Goldstein. 1998. Extending the range of rate constant available from BIACORE: interpreting mass transport-influenced binding data. *Biophys. J.* 75: 583–594.
30. Perelson, A. S. 1984. Some mathematical models of receptor clustering by multivalent ligands. *In* Cell Surface Dynamics. A. S. Perelson, C. DeLisi, and F. W. Wiegel, editors. Marcel Dekker, New York. 223–276.
31. Hammes, G. G. 2000. Thermodynamics and Kinetics for the Biological Sciences. Wiley Interscience, New York.
32. Vernazza, P. L., B. L. Gilliam, J. Dyer, S. A. Fiscus, J. J. Eron, A. C. Frank, and M. S. Cohen. 1997. Quantification of HIV in semen: correlation with antiviral treatment and immune status. *AIDS.* 11: 987–993.
33. Tachet, A., E. Dulioust, D. Salmon, M. De Almeida, S. Rivalland, L. Finkielsztejn, I. Heard, P. Jouannet, D. Sicard, and C. Rouzioux. 1999. Detection and quantification of HIV-1 in semen: identification of a subpopulation of men at high potential risk of viral sexual transmission. *AIDS.* 13:823–831.
34. Owen, D. H., and D. F. Katz. 2005. A review of the physical and chemical properties of human semen and the formulation of a semen simulant. *J. Androl.* 26:459–469.
35. Truskey, G. A., F. Yuan, and D. F. Katz. 2004. Transport Phenomena in Biological Systems. Pearson Prentice Hall, Upper Saddle River, NJ.
36. Amsden, B. 1998. Solute diffusion within hydrogels. Mechanisms and models. *Macromolecules.* 31:8382–8395.
37. Sassi, A. B., K. D. McCullough, M. R. Cost, S. L. Hillier, and L. C. Rohan. 2004. Permeability of tritiated water through human cervical and vaginal tissue. *J. Pharm. Sci.* 93:2009–2016.
38. Birudaraj, R., B. Berner, S. Shen, and X. Li. 2005. Buccal permeation of buspirone: mechanistic studies on transport pathways. *J. Pharm. Sci.* 94:70–78.
39. Chen, L.-L. H., D. J. Chetty, and Y. W. Chien. 1999. A mechanistic analysis to characterize oramucosal permeation properties. *Int. J. Pharm.* 184:63–72.
40. Tirucherai, G. S., C. Dias, and A. K. Mitra. 2002. Corneal permeation of Ganciclovir: mechanism of Glanciclovir permeation enhancement by acyl ester prodrug design. *J. Ocul. Pharmacol. Ther.* 18: 535–548.
41. Hoogstraate, A. J., C. Cullander, J. F. Nagelkerke, S. Senel, J. C. Verhoef, H. E. Junginger, and H. E. Bodde. 1994. Diffusion rates and transport pathways of fluorescein isothiocyanate (FITC)-labeled model compounds through buccal epithelium. *Pharm. Res.* 11:83–89.
42. Barnhart, K., A. Izquierdo, E. Pretorius, D. Shera, M. Shabbout, and A. Shaunik. 2006. Baseline dimensions of the human vagina. *Hum. Reprod.* 21:1618–1622.
43. Owen, D. H., J. J. Peters, and D. F. Katz. 2001. Comparison of the rheological properties of Advantage-S and Replens. *Contraception.* 64: 393–396.
44. Kilmarx, P. H., and L. Paxton. 2003. Need for a true placebo for vaginal microbicide efficacy trials. *Lancet.* 361:785–786.
45. Tien, D., R. L. Schnaare, F. Kang, G. Cohl, T. J. McCormick, T. R. Moench, G. Doncel, K. Watson, R. W. J. Buckheit, M. G. Lewis, J. Schwartz, K. Douville, and J. W. Romano. 2005. In vitro and in vivo characterization of a potential universal placebo designed for use in vaginal microbicide clinical trials. *AIDS Res. Hum. Retroviruses.* 21: 845–853.